INSTITUTE OF PHYSICS PUBLISHING NANOTECHNOLOGY
Nanotechnology **17** (2006) 3909–3914 doi:10.1088/0957-4484/17/15/049

An investigation into the structural features and thermal conductivity of silicon nanoparticles using molecular dynamics simulations

Kuan-Chuan Fang[1], Cheng-I Weng[1,2,4] and Shin-Pon Ju[3]

[1] Department of Mechanical Engineering, National Cheng Kung University, Tainan, Taiwan, Republic of China
[2] Fo Guang University, Jiaushi Shiang, Ilan, Taiwan, Republic of China
[3] Department of Mechanical and Electro-Mechanical Engineering, Center for Nanoscience and Nanotechnology, National Sun Yat-Sen University, Kaohsiung, Taiwan, Republic of China

E-mail: n1890110@ccmail.ncku.edu.tw (K-C Fang), weng@mail.ncku.edu.tw and jushin-pon@mail.nsysu.edu.tw

Received 5 May 2006, in final form 20 June 2006
Published 11 July 2006
Online at stacks.iop.org/Nano/17/3909

Abstract
The structural features and thermal conductivity of silicon nanoparticles of diameter 2–12 nm are studied in a series of molecular dynamics simulations based on the Stilling–Weber (SW) potential model. The results show that the cohesive energy of the particles increases monotonically with an increasing particle size and is independent of the temperature. It is found that particles with a diameter of 2 nm have a heavily reconstructed geometry which generates lattice imperfections. The thermal conductivity of the nanoscale silicon particles increases linearly with their diameter and is two orders of magnitude lower than that of bulk silicon. The low thermal conductivity of the smallest nanoparticles is thought to be the result of particle boundary and lattice imperfections produced during fabrication, which reduce the phonon mean free path (MFP). Finally, it is found that the influence of the temperature on the thermal conductivity decreases significantly as the temperature increases. Again, this is thought to be the result of a reduced phonon MFP at elevated temperatures.

(Some figures in this article are in colour only in the electronic version)

1. Introduction

As the physical dimensions of a system become comparable to or smaller than the characteristic scale of the physical phenomenon of interest, excellent properties commonly arise. For example, the quantum phenomena in zero-dimensional (0D) structures such as nanoparticles are more significant than those in the bulk system. Nanoparticles have many exciting potential applications, including in nanoscale electronic devices such as semiconductor quantum dots (QDs) [1, 2]. These nanoparticles represent a new class of material which shows fingerprints of the properties observed in atomic or molecular physics on the one hand and elements of condensed matter physics on the other. Furthermore, nanoparticles contain a large percentage of surface atoms, which render them ideal for a variety of novel electronic and optoelectronic applications [3, 4]. Bond contractions caused by the low coordination of these surface atoms have been observed on the extended surfaces of many systems [5]. These bond contractions are 'tunable' through the particle size, because small particles behave as matter under high pressure and enable the formation of new structures [6]. Therefore, the physical and chemical properties of nanoparticles have attracted considerable attention in recent years.

[4] Author to whom any correspondence should be addressed.

Table 1. Parameters used in Stillinger–Weber (SW) potential.

ε (eV)	A	B	σ (Å)	p	q	a (Å)	λ	γ
2.168 26	7.049 556 277	0.602 224 5584	2.0951	4	0	1.80	21.0	1.20

Regarding the mechanical properties of nanoparticles, hardness values of up to 50 GPa have been measured for silicon nanospheres, which is fully four times greater than the value of 12 GPa for bulk silicon [7]. Meanwhile, it has been reported that mechanically milled iron powders with small volumes have a hardness of 8.4 GPa [8]. A richness of mechanical phenomena has been observed in small-scale systems, including very high internal stresses, which offer considerable potential for the design of super-hard materials. Furthermore, solid particles have been dispersed in traditional heat transfer fluids to enhance their effective thermal conductivity [9, 10]. When crystalline solids are confined to the nanometre scale, their thermal conductivity can be significantly reduced by boundary scattering effects, changes in the phonon dispersion relation, and quantization of the phonon transport. It has been reported that the thermal conductivity of these crystalline solids may be reduced by two orders of magnitude compared to that of the bulk crystal material. The low thermal conductivity property of nanoparticles renders them ideal candidates for the design of new thermal resistant materials.

To further the development of future nanoparticle applications, it is necessary that the structural features and thermal conductivity properties of nanoparticles of different sizes be well understood. However, it is difficult to explore the size-dependent nature of the nanoparticle properties using direct experimental approaches. Fortunately, molecular dynamics (MD) simulations can provide detailed insights into the physics of these particles when seeking to clarify the dependence of their thermodynamic behaviour on their size. This simulation method describes the atomic motions of the constituent particles of a material based on the assumption that the laws of classic mechanics still apply on the atomic scale [11]. The benefits of the MD approach become increasingly apparent as the characteristic size of the system decreases. MD simulations have been employed successfully to study the properties of silicon nanoparticles [12]. The results showed that the interior atoms of 480-atom clusters exhibited bulk-like characteristics over a wide temperatures range ($600 < T < 2000$). Additionally, the average surface energy of the cluster was found to be dependent on the cluster size. However, previous studies generally considered silicon particles with at most several thousands atoms or less [12–14]. A review of the literature suggests that few attempts have been made to investigate the properties of larger particles typical of those used in nanoscale-size devices.

Consequently, this study conducts classical MD simulations to determine the structural features and thermal conductivities of silicon nanoparticles with diameters ranging from 2 to 12 nm (corresponding to particle sizes of 191–45 214 atoms). A particular focus is placed on the size-dependent characteristics of the particles' structural features and thermal conductivities under temperatures ranging from 25 to 500 K.

Table 2. Simulation cases for silicon nanoparticles in this study.

Case	Cutoff diameter (nm)	Particle size (N)
1	2.0	191
2	3.0	705
3	4.0	1 707
4	5.0	3 265
5	6.0	5 707
6	7.0	9 041
7	8.0	13 407
8	9.0	19 129
9	10.0	26 167
10	11.0	34 937
11	12.0	45 215

2. Methodology

The current MD simulations were conducted using the silicon potential model proposed by Stillinger and Weber (SW) [15]. This empirical potential function contains two- and three-body interactions which take into consideration the directional characteristics of the covalent bonding. The SW empirical interatomic potential function has the form:

$$V = \sum_{i,j} V_2(r_i, r_j) + \sum_{i,j,k} V_3(r_i, r_j, r_k). \tag{1}$$

The two-body term, $V_2(r_i, r_j)$, is given by:

$$V_2(r_i, r_j) = \begin{cases} A(Br^{-p} - r^{-q}) \exp[(r-a)^{-1}], & r < a \\ 0, & r \geqslant a \end{cases} \tag{2}$$

and the three-body term, $V_3(r_i, r_j, r_k)$, is expressed as:

$$V_3(r_i, r_j, r_k) = h(r_{ij}, r_{ik}, \theta_{jik}) + h(r_{ji}, r_{jk}, \theta_{ijk}) + h(r_{ki}, r_{kj}, \theta_{ikj}) \tag{3}$$

where:

$$h(r_{ij}, r_{ik}, \theta_{jik}) = \lambda \exp[\gamma(r_{ij} - a)^{-1} + \gamma(r_{ik} - a)^{-1}] \times \cos\left(\theta_{jik} + \tfrac{1}{3}\right) \tag{4}$$

in which $\vec{r_{ij}}$ is the vector pointing from atom i to atom j, with $r_{ij} = |\vec{r_{ij}}|$, and θ_{ijk} is the angle between vectors $\vec{r_{ij}}$ and $\vec{r_{ik}}$. The constants A, B, p, q, a, λ and γ are all positive and correspond to the case of the most stable diamond structure. However, the melting point, cohesive energy and lattice parameter inferred for the tentative interaction by MD simulation must be in reasonable accord with the experimental values. The Stillinger–Weber potential parameters adopted in the present study are presented in table 1 [15].

The initial geometries of the nanoparticles considered in this study were constructed from a large block of silicon with a diamond structure by using various spherical cutoff diameters ranging from 2 to 12 nm centred at a tetrahedral interstitial site. The particle parameters used in the current simulations are presented in table 2.

The MD simulations were performed under conditions of a constant temperature (T), a constant shape (h), and a constant particle number (ThN). Since the phonon mean free path (MFP) in crystalline solids is much longer than that in amorphous solids, it is particularly challenging to calculate the thermal conductivity of solid-phase crystalline systems. Therefore, to simulate the total phonon transport properties of the crystalline particles, all of the particles were initially relaxed at a high temperature ($T = 600$ K) for 5×10^5 time steps (where one time step d$t = 0.5$ fs). This precaution was taken to remove any angular momentum and unrealistic, artificial surface effects from the system in the equilibrium state. The particles were then annealed to the desired target temperature over 5×10^5 time steps. Simulation runs to obtain the nanoparticle properties were performed at a fixed temperature, and the total angular momentum of the particle motion was reset to zero after each time step by transforming the velocities in order to evaluate the transport properties. To obtain reliable results for the particle characteristics, the simulations were performed for 1×10^6 time steps (500 ps) to ensure a reasonable statistical averaging result after the equilibrium process. For comparison purposes, the bulk system, modelled with 2744 atoms in the cube, was also simulated and the cohesive energy and bulk thermal conductivity computed under constant temperature and constant volume (NVT) conditions with periodic boundary conditions.

Due to their large surface-to-volume ratio, the properties of nanoparticles are different from those of the bulk system. The approach of the particle properties to the bulk properties as the particle size is increased is generally specific to the properties of interest. Previous studies of the properties of nanoparticles have suggested that the particle properties depend on the particle's cohesive energy and surface energy. The relative contributions of these two energies can be expressed as:

$$E_\mathrm{p} = E_\mathrm{b} + E_\mathrm{s} \tag{5}$$

where E_p, E_b and E_s represent the particle cohesive energy, the bulk binding energy and the particle surface energy, respectively.

In this study, the structural characterization of the particles was performed by calculating their radial distribution function (RDF). The RDF, $g(r)$, is a fundamental parameter used to describe the structural characterization of amorphous and crystalline states and has the form:

$$g(r) = \frac{V}{N}\left\langle \frac{\sum_{i=1}^{N_i} n_i(r)}{4\pi r^2 \Delta r} \right\rangle \tag{6}$$

where $g(r)$ is the probability of finding an atom within a distance ranging from r to $r + \Delta r$, where Δr is the spatial step of the calculation, V is the simulated volume of the particle, N is the number of atoms in the particle, and n_i is the average number of atoms around the ith atom in the spherical shell extending from r to $r + \Delta r$.

In general, two methods are commonly employed when using simulation approaches to determine the thermal conductivity of the system of interest. The first method is to subject the simulated system to an explicit external perturbation (e.g. a temperature gradient) and to calculate the steady-state response. Alternatively, the Green–Kubo (GK) relation can be applied, i.e. the relation between the thermal conductivity and correlation functions involving fluxes of conserved quantities [16]. The present study adopts the latter approach to calculate the thermal conductivities of the current silicon nanoparticles.

The thermal conductivity coefficient provides an indication of the heat transport in a system. The correlation function is obtained from the heat current and is a collective property of the particle. The GK formula is given by:

$$\lambda = \frac{1}{V k_\mathrm{B} T_0^2} \int_0^\infty \langle J(t) J(0) \rangle \, \mathrm{d}t \tag{7}$$

where:

$$J(t) = \sum_{i=1}^{N} \sum_{j=1, j\neq i}^{N} \left[\tfrac{1}{2} r_{ij} \cdot (F_{ij} \cdot v_i) + \tfrac{1}{6} \sum_{k=1, k\neq i,j}^{N} (r_{ij} + r_{jk}) \times (F_{ijk} \cdot v_i) \right] \tag{8}$$

where $J(t)$ denotes the heat flux vector. In equations (7) and (8), V is the volume of the particle, T_0 is the equilibrium temperature, k_B is the Boltzmann constant, r_{ij} is given by $r_{ij} = |r_i - r_j|$, and F_{ij} and F_{ijk} are the two- and three-body forces, respectively. In the present study, the statistical precision of the thermal conductivity computation is improved by averaging over all three components (λ_x, λ_y, λ_z).

In the simulations, the particle radius is given by:

$$R_\mathrm{C} = R_\mathrm{g}\sqrt{5/3} + R_\mathrm{Si} \tag{9}$$

where R_g is the radius of gyration and is determined from:

$$R_\mathrm{g}^2 = \left(\frac{1}{N}\right) \sum_i (R_i - R_\mathrm{cm})^2 \tag{10}$$

where the atom radius, R_Si, is one quarter of the interatomic distance in the bulk system, i.e. $R_\mathrm{Si} = 1.3575$ Å.

3. Results and discussion

Previous studies of the size-dependent nature of nanoparticle properties have generally expressed the particle's size in terms of the number of atoms it contains. However, this measure is very difficult to evaluate experimentally. Conversely, the particle diameter can be measured relatively easily, and is therefore used as the particle size indicator in the present study. Figure 1 shows the variation in the cohesive energy with the particle size at temperatures of 100, 300 and 500 K, respectively. It can be seen that the cohesive energy increases monotonically with increasing particle size. This result is in agreement with experimental observations of small silicon particles [11, 17]. The three solid lines indicate the best fit of the simulation results to a linear function of $1/d$, where d is the particle diameter. In practice, $1/d$ is equivalent to the surface-to-volume ratio. Hence, figure 1 shows that the cohesive energy of the nanoparticles scales linearly with the surface-to-volume ratio. Furthermore, it can be inferred that the approach of the particles' cohesive energy to a bulk behaviour is independent of the temperature.

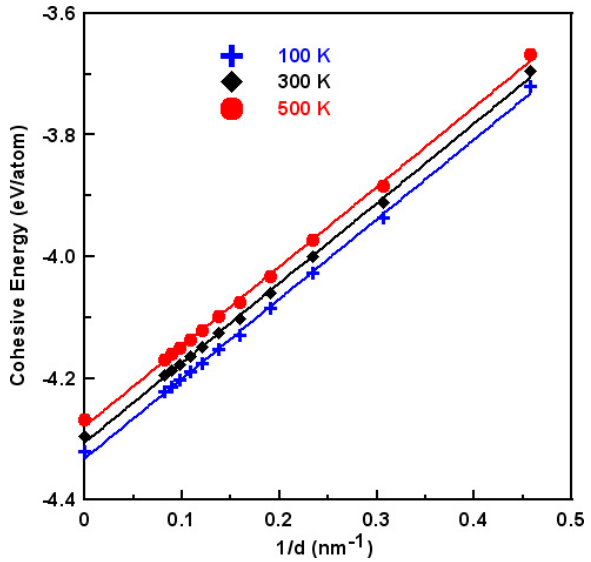

Figure 1. Dependence of cohesive energy per atom on particle size (d denotes particle diameter) at temperatures of 100, 300 and 500 K. Solid lines indicate the best fit of data to a linear function of $1/d$.

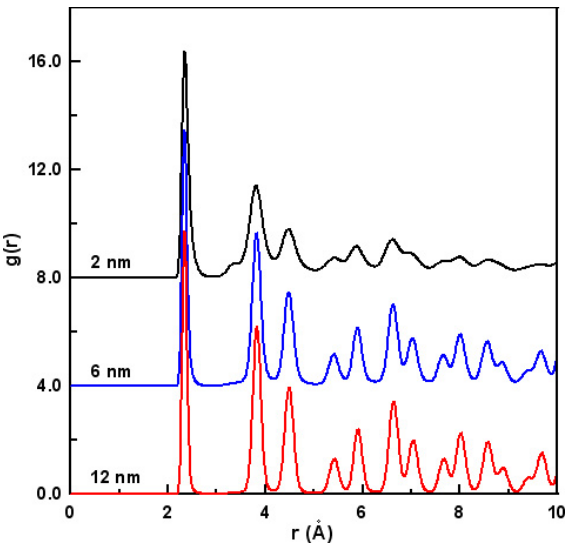

Figure 2. Radial distribution function, $g(r)$, for particles of diameter 2, 6 and 12 nm, respectively, at 300 K.

Table 3 shows the variation in the properties of the silicon nanoparticles at a constant temperature of 300 K as a function of the particle size. It is observed that the cohesive energy becomes increasingly negative as the particle size increases, implying that larger particles have a greater stability. Because the small silicon particle revealed more suspension bond and a high activation energy, the atoms on the particle's surface reconstructed to a more stable structure. This result can be explained by the reduced surface-to-volume ratio and the surface reconstruction behaviour as the particle size increases. The cohesive energy of bulk silicon at 300 K is also reported in table 3. The calculated value of −4.30 eV/atom is consistent with the experimentally obtained value of −4.63 eV/atom (0 K) [18]. The surface energy is one of the most important properties in understanding the optical and chemical properties of nanostructured materials. Table 3 summarizes the surface energy of the current particles at 300 K, as calculated from equation (5). It can be seen that the surface energy increases as the particle size decreases. This result can be attributed to the more incomplete bond structure of the smaller particles compared with that of their larger counterparts. In other words, a higher chemical activity exists in the smaller particles.

Figure 2 presents the RDF results for nanoparticles with diameters of 2, 6 and 12 nm, respectively, at a temperature of 300 K. The RDF curves all exhibit a crystalline peak characteristic, which suggests that the particles have a crystal-like structure. It is seen that the first and second main peaks are located at 2.35 and 3.86 Å, respectively. This result is consistent with the findings of a previous simulation study for bulk silicon [19]. Significantly, a small peak is observed at 3.49 Å between the first and the second peaks of the RDF for the particle with a diameter of 2 nm. This peak is not the characteristic neighbour peak observed in crystalline silicon. More likely, the presence of this peak suggests that the small particle has a heavily reconstructed geometry, which generates lattice imperfections.

Table 3. Properties of silicon nanoparticles at 300 K as a function of particle diameter.

Cutoff diameter (nm)	Particle diameter (nm)	Surface energy (kJ mol^{-1})	Cohesive energy (eV/atom)
2.0	2.19	57.97	−3.69
3.0	3.26	37.10	−3.91
4.0	4.27	28.42	−4.00
5.0	5.26	22.74	−4.06
6.0	6.27	18.57	−4.10
7.0	7.28	16.30	−4.13
8.0	8.26	14.12	−4.15
9.0	9.27	12.71	−4.16
10.0	10.27	11.41	−4.18
11.0	11.28	10.35	−4.19
12.0	12.27	9.56	−4.20
Bulk (simulation)			−4.30
Bulk (experiment)[a]			−4.63

[a] Reference [18] (for the cohesive energy at 0 K).

Figures 3(a) and (b) show the heat current correlation functions at 300 K for bulk crystal silicon and the silicon particle with a diameter of 6 nm, respectively. The insets reveal that both heat current correlation functions decay rapidly in the initial period of 0.2 ps. This effect is related to the presence of high-frequency optical modes, which contribute little to the thermal conductivity, as argued in a previous simulation study [20]. However, over a longer time period, the heat current correlation function for the bulk crystal silicon decays more slowly than that of the nanoparticle. This slow decay behaviour can be attributed to low-frequency acoustic modes. Conversely, the heat current correlation function for the particle with a diameter of 6 nm decays to zero within 0.6 ps, indicating that very few low-frequency acoustic modes exist in silicon nanoparticles.

Based on the macroscopic law of relaxation and Onsager's postulate for microscopic thermal fluctuation, the heat correlation function can be expressed in the form of a double

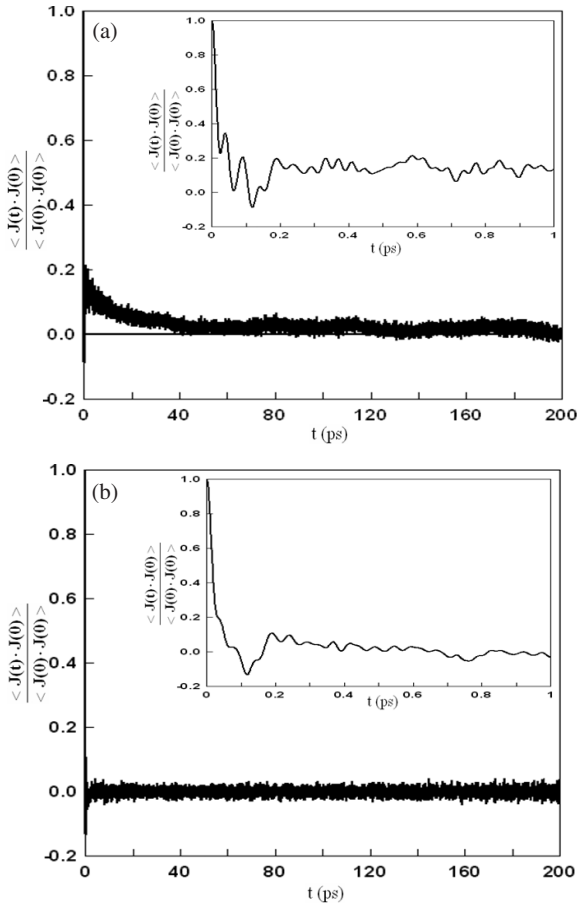

Figure 3. Heat current correlation functions for: (a) bulk system, and (b) a particle with diameter of 6 nm at 300 K. Insets show the same data in the short-time region.

exponential function, i.e.

$$\langle J(t)J(0)\rangle = A_{\mathrm{o}}\exp(-t/\tau_{\mathrm{o}}) + A_{\mathrm{a}}\exp(-t/\tau_{\mathrm{a}}) \qquad (11)$$

where subscripts o and a denote fast optical modes and slow acoustic modes, respectively. The thermal conductivity is then given by:

$$\lambda = \frac{1}{k_{\mathrm{B}}T^2V}(A_{\mathrm{o}}\tau_{\mathrm{o}} + A_{\mathrm{a}}\tau_{\mathrm{a}}) \qquad (12)$$

where the parameters A_{o}, τ_{o}, A_{a} and τ_{a} are derived from the first 3 ps using the Mazquazlt–Levenberg nonlinear least-squares method. A non-exponential decay of the correlation function is quite common in most physical processes. Therefore, to ensure a meaningful result, the present computations used an averaging process to obtain the thermal conductivity results. Figures 3(a) and (b) show that the heat current correlation function decays to approximately zero within 130 ps in the bulk crystal silicon and within the nanoparticle. Hence, the thermal conductivity of the current particles was obtained by applying the direct integration method out to a time of 200 ps.

Figure 4 illustrates the dependence of the thermal conductivity on the particle size. It is observed that the calculated thermal conductivities of the particles are lower than that of the bulk by approximately two orders of magnitude.

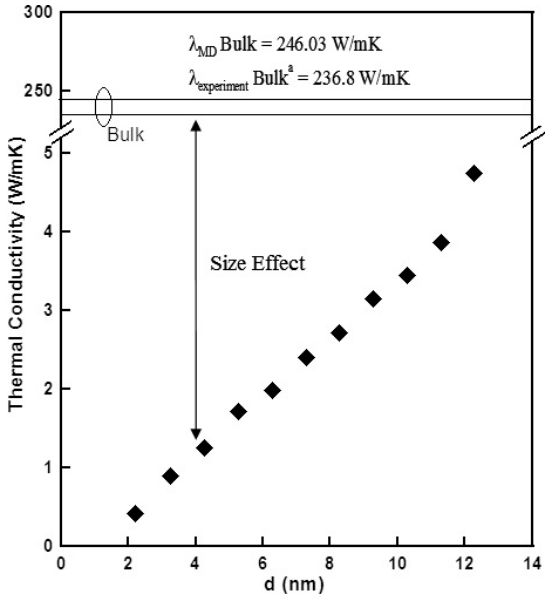

Figure 4. Dependence of thermal conductivity on particle size at 300 K. The simulated thermal conductivity of the bulk (λ_{MD}Bulk) and the experimental thermal conductivity of the bulk ($\lambda_{\mathrm{experiment}}$Bulk) are shown for reference [22].

Furthermore, the thermal conductivity of the smallest particle is lower by one order of magnitude than that of the largest particle. To obtain a better understanding of the heat conduction mechanism in the nanoparticles, the lattice thermal conductivity can be determined from the kinetic theory of gases, i.e.

$$\lambda = \tfrac{1}{3}CvL \qquad (13)$$

where C is the heat capacity per volume, v is the phonon velocity and L is the phonon mean free path (MFP). In brief, substituting d for L in equation (13) yields the proportional relationship $\lambda \propto d$, which is consistent with the simulation results. The phonon MFP in small particles may be reduced by phonon–phonon scattering, scattering at the boundaries and lattice imperfections arising from the particle fabrication process [21]. However, the relationship between the particle size and its thermal conductivity is linearly dependent for the particle size which is over 2 nm, as shown in figure 4. It can be seen that lattice imperfections in smaller nanoparticles cannot remarkably influence the thermal conductivity. This indicates that the phonon–phonon scattering at the boundary can be more remarkable than that at the lattice imperfections. Though lattice imperfections are readily formed in small particles, as shown in figure 2, the thermal conductivity of nanoparticles is mainly subject to its size. Therefore, the results suggest that the thermal conductivity of nanoscale silicon particles is subject to a size-dependent effect.

Finally, figure 5 presents the variation in the thermal conductivity of the particle with a diameter of 6 nm as a function of temperature over the range 25–500 K. It can be seen that the thermal conductivity remains approximately constant between 100 and 500 K. This indicates that the phonon MFP is significantly reduced at higher temperatures in particles with a diameter of the order of several nanometres.

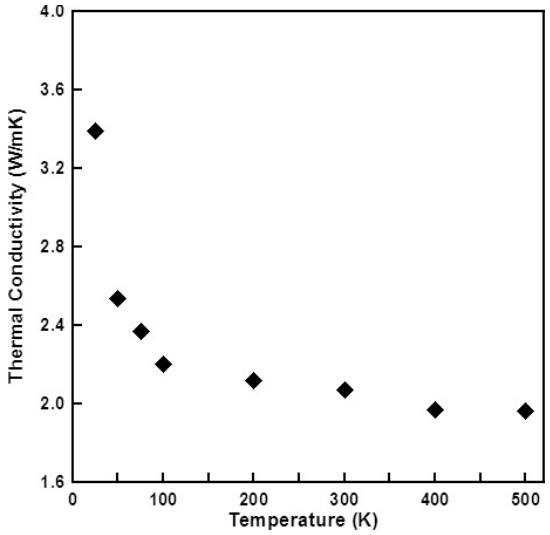

Figure 5. Variation of thermal conductivity of a particle with a diameter of 6 nm with temperature.

4. Conclusion

This study has employed MD simulations based on the Stilling–Weber (SW) potential model to investigate the effect of temperature on the structural features and thermal conductivity of silicon nanoparticles with diameters of 2–12 nm. The results have shown that the particle cohesive energy can be fitted to a linear function of $1/d$, where d is the particle diameter, and is independent of the temperature. Additionally, the RDF results have indicated that lattice imperfections are generated in small particles (e.g. 2 nm diameter). The thermal conductivity of silicon particles increases linearly with an increasing particle diameter, but is constrained in smaller particles by lattice imperfections, which cause a reduction in the phonon MFP. Finally, it has been shown that the thermal conductivity decreases rapidly as the temperature increases from 25 to 100 K, but then remains stable as the temperature is increased further. Again, this is thought to be the result of a reduced phonon MFP at higher temperatures.

Acknowledgment

The authors gratefully acknowledge the financial support provided to this study by the National Science Council of the Republic of China under Grant No NSC94-2212-E-006-001.

References

[1] Lazarenkova O and Balandin A 2001 *J. Appl. Phys.* **89** 5509
[2] Khitun A, Liu J and Wang K L 2004 *Appl. Phys. Lett.* **84** 1764
[3] Huffaker D L, Park G, Zou Z, Schekin O B and Deppe D G 1998 *Appl. Phys. Lett.* **73** 2564
[4] Lin J L, Tang Y S, Wang K L, Radetic T and Gronsky R 1999 *Appl. Phys. Lett.* **74** 1863
[5] Apai G, Hamiton J F, Stohr J and Thompson A 1979 *Phys. Rev. Lett.* **43** 165
[6] Tomanek D and Schluter M A 1987 *Phys. Rev.* B **36** 1208
[7] Gerberich W W, Mook W M, Perrey C R, Carter C B, Baskes M I, Mukherjee R, Gidwani A, Heberlein J, McMurry P H and Girshick S L 2003 *J. Mech. Phys. Solids* **51** 979
[8] Murayama M, Howe J M, Hidaka H and Tokai S 2002 *Science* **295** 2433
[9] Eastman J A, Choi S U S, Li S, Yu W and Thompson L J 2001 *Appl. Phys. Lett.* **78** 718
[10] Ren Y, Xie H and Cai A 2005 *J. Phys. D: Appl. Phys.* **38** 3958
[11] Frenkel D and Smit B 1996 *Understanding Molecular Simulation from Algorithms to Applications* (New York: Academic)
[12] Zachariah M R, Carrier M J and Estela B B 1996 *J. Phys. Chem.* **100** 14856
[13] Fang K C and Weng C I 2005 *Nanotechnology* **16** 250
[14] Hayashi R, Tanaka K, Horiguchi S and Hiwatari Y 2001 *Diamond Relat. Mater.* **10** 1224
[15] Stillinger F H and Weber T A 1985 *Phys. Rev.* B **31** 5262
[16] Allen M P and Tildesley D J 1987 *Computer Simulation of Liquids* (Oxford: Clarendon)
[17] Kaxiras E and Jackson K 1993 *Phys. Rev. Lett.* **71** 727
[18] Edwards B 1997 *Phys. Rev.* B **55** 1528
[19] Ishimaru M 2001 *J. Phys.: Condens. Matter* **13** 4181
[20] Che J, Cagin T, Deng W and Goddard W A 2000 *J. Chem. Phys.* **113** 6888
[21] Volz S G and Chen G 1999 *Appl. Phys. Lett.* **75** 2056
[22] Capinski W S, Maris H J, Bauser E, Silier I, Asen-Palmer M, Ruf T, Cardona M and Gmelin E 1997 *Appl. Phys. Lett.* **71** 2109